

Effects of CO₂ laser irradiation on matrix-rich biofilm development formation—an in vitro study

Bruna Raquel Zancopé¹, Vanessa B. Dainezi¹,
Marinês Nobre-dos-Santos¹, Sillas Duarte Jr.², Vanessa Pardi³ and
Ramiro M. Murata⁴

¹ Department of Pediatric Dentistry, Piracicaba Dental School, University of Campinas-UNICAMP, Piracicaba, São Paulo, Brazil

² Division of Restorative Sciences, Ostrow School of Dentistry of University of Southern California, Los Angeles, California, USA

³ Division of Periodontology, Diagnostic Sciences and Dental Hygiene, Ostrow School of Dentistry of University of Southern California, Los Angeles, California, USA

⁴ Department of Foundational Sciences, School of Dental Medicine, East Carolina University, Greenville, North Carolina, USA

ABSTRACT

Background: A carbon dioxide (CO₂) laser has been used to morphologically and chemically modify the dental enamel surface as well as to make it more resistant to demineralization. Despite a variety of experiments demonstrating the inhibitory effect of a CO₂ laser in reduce enamel demineralization, little is known about the effect of surface irradiated on bacterial growth. Thus, this in vitro study was preformed to evaluate the biofilm formation on enamel previously irradiated with a CO₂ laser ($\lambda = 10.6 \mu\text{M}$).

Methods: For this in vitro study, 96 specimens of bovine enamel were employed, which were divided into two groups (n = 48): 1) Control-non-irradiated surface and 2) Irradiated enamel surface. Biofilms were grown on the enamel specimens by one, three and five days under intermittent cariogenic condition in the irradiated and non-irradiated surface. In each assessment time, the biofilm were evaluated by dry weigh, counting the number of viable colonies and, in fifth day, were evaluated by polysaccharides analysis, quantitative real time Polymerase Chain Reaction (PCR) as well as by contact angle. In addition, the morphology of biofilms was characterized by fluorescence microscopy and field emission scanning electron microscopy (FESEM).

Initially, the assumptions of equal variances and normal distribution of errors were conferred and the results are analyzed statistically by t-test and Mann Whitney test. **Results:** The mean of log CFU/mL obtained for the one-day biofilm evaluation showed that there is statistical difference between the experimental groups. When biofilms were exposed to the CO₂ laser, CFU/mL and CFU/dry weight in three day was reduced significantly compared with control group. The difference in the genes expression (Glucosyltransferases (gtfB) and Glucan-binding protein (gbpB)) and polysaccharides was not statically significant. Contact angle was increased relative to control when the surface was irradiated with the CO₂ laser. Similar morphology was also visible with both treatments; however, the irradiated group revealed evidence of melting and fusion in the specimens.

Conclusion: In conclusion, CO₂ laser irradiation modifies the energy surface and disrupts the initial biofilm formation.

Submitted 5 March 2016
Accepted 17 August 2016
Published 1 November 2016

Corresponding author
Ramiro M. Murata,
muratar16@ecu.edu

Academic editor
Praveen Arany

Additional Information and
Declarations can be found on
page 12

DOI 10.7717/peerj.2458

© Copyright
2016 Zancopé et al.

Distributed under
Creative Commons CC-BY 4.0

OPEN ACCESS

Subjects Biochemistry, Dentistry

Keywords Lasers, Biofilm, Caries, Prevention & control

INTRODUCTION

Dental caries, a biofilm-related disease, remains among the most prevalent human infections disease affecting both children and adults worldwide (Do, 2012; Dye et al., 2008; Marcenes et al., 2013). Despite its decline over the last decades primarily due to the widespread use of fluoride compounds, caries disease activity in children is as high as 60–70% (Murata & Pardi, 2007; Taubman & Nash, 2006; García-Godoy & Hicks, 2008; Greene, 2005; Hausen, 1997; Peterson, 2003). Colonization of tooth surfaces by *mutans streptococci* and its interaction with constituents from the host's diet is associated with the etiology and pathogenesis of dental caries in humans (Bowen, 2002; Marsh, 2003). Although dental biofilms are composed of diverse and complex oral microorganisms, *Streptococcus mutans* is considered the primary etiologic agent of dental caries, which has an important role in the initiation and progression of the dental caries (Loesche, 1986; Wang et al., 2013), as it uses carbohydrates, such sucrose, to synthesize extracellular polysaccharides and can survive under low pH conditions, leading to enamel demineralization (Rölla, 1989).

Laser therapy has been studied as a promising alternative in the prevention of caries. Different types of lasers such as Nd:YAG, Argon, Er:YAG and carbon dioxide (CO₂) have been studied for their potential use in dentistry. The use of high-power lasers has been suggested as the treatment of tooth enamel in order to obtain more resistant surfaces to acids produced by cariogenic bacteria (Featherstone et al., 1991; Featherstone et al., 1998; Hsu et al., 2000; Kantorowitz, Featherstone & Fried, 1998). A study conducted by Armengol et al. (2003) showed that morphological changes on enamel and dentin were greater when Er:YAG laser and Nd:YAP laser were employed, which was associated with a greater free surface energy. Intriguingly, Venault et al. (2014) reported that the coating of hydroxyapatite with a polyethyleneimine (PEI) polymer inhibited the adsorption and showed a 70% inhibition of oral bacterial adhesion on human teeth. However, the applicability of superhydrophobic and superhydrophilic surfaces in the dental field remains to be investigated. The conventional wisdom is that a reduction of surface roughness and surface free energy of a dental material coincides with a decrease in microbial adherence and proliferation (Buergers et al., 2009; Teughels et al., 2006). These results suggest that surface parameters such as the chemical composition and topography might be key parameters for optimizing the enamel surface properties in order to reduce biofilm formation on their surfaces.

The CO₂ laser acts on enamel demineralization to reduce the acid solubility. Previous studies have also shown significant inhibition of enamel demineralization following treatment with a CO₂ laser (Hsu et al., 2001; Nobre-dos-Santos, Featherstone & Fried, 2001; Rodrigues, dos Santos & Featherstone, 2006; Steiner-Oliveira et al., 2006; Tagliaferro et al., 2007). There are several hypotheses that attempt to explain the mechanisms by which a CO₂ laser inhibits tooth enamel demineralization. One

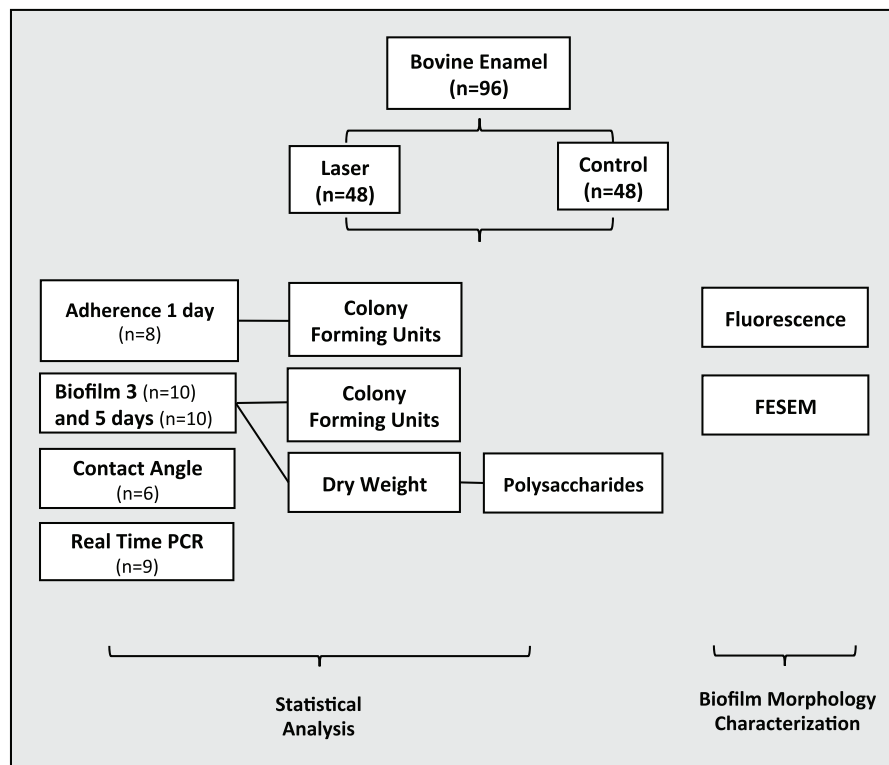


Figure 1 Flowchart of the experimental design of the study.

possible explanation is based on reducing enamel solubility caused by the melting and recrystallization of hydroxyapatite crystals (Nelson *et al.*, 1986). However, there is no report in scientific literature showing whether these morphological alterations promoted by laser irradiation could change the energy surface and consequently to modify the development of biofilm enamel surface. Thereby, the aim of this study was to evaluate the biofilm formation on enamel previously irradiated with a CO₂ laser ($\lambda = 10.6 \mu\text{M}$).

MATERIAL AND METHODS

Experimental design

Ninety-six dental enamel specimens were previously prepared were randomly allocated in two groups ($n = 48$): 1) Control-non-irradiated surface and 2) Irradiated enamel surface. Biofilms were grown on the enamel specimens by one, three and five days under intermittent cariogenic condition in the irradiated and non-irradiated surface. The following analyses were performed: adherence test with one-day biofilm formation ($n = 8$), bacterial viability, colony forming units–CFU/mg of biofilm dry weight, dry weight and polysaccharides analysis with three-day ($n = 10$) and five-day ($n = 10$) biofilm formation. Real time Polymerase Chain Reaction (PCR) ($n = 9$) and Contact angle ($n = 6$). Morphological surface changes of three specimens of each group were examined by Field Emission Scanning Electron Microscopy (FESEM) and by fluorescence microscopy (Fig. 1).

Tooth selection and sample preparation, experimental model

To perform this in vitro study, 96 sound bovine incisors that were free from caries, macroscopic cracks, abrasions as well as staining assessed by visual examination, were stored in a 0.1% thymol solution, and sectioned mesiodistally using a water-cooled diamond saw in a cutting machine (Isomet; Buehler, Lake Bluff, IL, USA). The tooth halves were polished for 30 s using a 5 μM alumina/water suspension micropolish (Instrumental, Jabaquara, SP, Brazil) to expose fresh enamel. The specimens were coated with an acid-resistant varnish leaving a window of 4 mm^2 of exposed enamel in the middle of the surface. The teeth were sterilized using oxide ethylene (Acecil Central Esterilizacao com Ind. Ltda de Campinas-SP, Campinas, Brasil).

Laser irradiation parameters

For this study, we based the irradiation parameters in a previous work by our group ([Steiner-Oliveira et al., 2006](#)) showing that 11.3 J/cm^2 was able to produce chemical and morphological changes that could reduce the acid reactivity of enamel without compromising pulp vitality. To perform enamel surface irradiation, a pulsed CO_2 laser at 10.6 μM wavelength (Union Medical Engineering Co. Model UM-L30; Yangju-si, Gyeonggi-Do, Korea) was used with the following parameters: 10-ms pulse duration, 10-ms of time off, 50-Hz repetition rate, beam diameter of 0.3-mm (according to laser manufacturer), single pulse fluence of 11.3 J/cm^2 and total fluence delivered to treated area of 300 J/cm^2 . The average power output was measured at 0.4 W using a power meter (Scientech 373 Model-37-3002; Scientech Inc., Boulder, CO, USA). To provide uniform coverage of enamel surface (4 mm^2), we used a X-Y positioning platform at a 10-mm distance from the tip of the handpiece to the enamel surface. The handpiece was positioned perpendicularly to the enamel surface, and we irradiated the samples once in each direction, slowly by manually moving the X-Y positioning platform horizontally and vertically, in order to promote homogeneous irradiation of the entire specimen experimental surface area.

Biofilm formation and analysis

Streptococcus mutans UA159 (ATCC 700610), a virulent cariogenic pathogen, was used for the biofilm study. Biofilms were grown in Brain Heart Infusion (BHI) broth containing 1% (w/v) sucrose and were kept undisturbed for 24 h to allow initial biofilm formation. Medium was replaced twice daily. Biofilms of *S. mutans* UA159 were formed on specimens of bovine enamel placed in 2 mL of medium containing 1% sucrose, in 24-well cell culture plates, at 37 °C, 5% CO_2 , for three and five days, which were dip-washed three times with Phosphate Buffered Saline (PBS) at the end of each experimental period. The biofilms were removed using a metallic spatula, immersed in a falcon tube with PBS and subjected to sonication using three 15 s pulses at an output of 7 W (Fisher Scientific, Sonic Dismembrator model 100; NH, USA). The suspension was used as previously described ([Duarte et al., 2006](#)) for dry weight, bacterial viability (colony forming units—CFU/mg of biofilm dry weight), and polysaccharide analyses (EPS-soluble, EPS-insoluble and intracellular polysaccharides—IPS) ([Duarte et al., 2011](#)).

S. mutans adherence test was performed in day 1 of biofilm formation. After that, the numbers of colonies were counted and the value of log CFU/mL was calculated (Branco-de-Almeida et al., 2011).

Dry weight and bacterial viability

Three volumes containing cold ethanol (-20°C) were added to 1 mL biofilm suspension, and the resulting precipitate was centrifuged (10,000 g for 10 min at 4°C). The supernatant was discarded, and the pellet was washed with cold ethanol, and then lyophilized and weighed (Duarte et al., 2006).

An aliquot (0.1 mL) of the homogenized suspension was serially diluted (1:10, 1:100, 1:1,000, 1:10,000, 1:100,000, 1:1,000,000) and plated on blood agar. The plates were incubated in 5% CO_2 at 37°C for 48 h, and the number of CFU mg⁻¹ of biofilm dry weight were determined (Murata et al., 2010).

Polysaccharide analysis

Soluble and insoluble extracellular polysaccharides (EPS-soluble and EPS-insoluble) were analyzed as previously described (Duarte et al., 2006). The polysaccharide content was expressed per mg of polysaccharide by dry weight of total biofilm. Briefly, an aliquot (2 mL) of the suspension was sonicated for 30 s pulses at an output of 7 W and centrifuged at 10,000 g for 10 min at 4°C . The supernatant was collected and the biofilm pellet was resuspended and washed in 5 mL of milli-Q water. This procedure was repeated three times. The supernatant was used for the EPS-soluble assay and biofilm pellet was used for the EPS-insoluble assay. All of the supernatants were pooled and three volumes of cold ethanol were added, and the resulting precipitate was collected by centrifugation and resuspended in 5 mL Milli-Q water; the total amount of carbohydrate was determined by the phenol—sulfuric acid method (Dubois et al., 1951). The EPS-insoluble was extracted using 1 N NaOH (1 mg biofilm dry weight/0.3 mL of 1 N NaOH) under agitation for 1 h at 37°C . The supernatant was collected by centrifugation, and the precipitate was resuspended again in 1N NaOH; this procedure was repeated three times. The total amount of carbohydrate was determined by colorimetric method with phenol sulfuric acid (Dubois et al., 1951).

Quantitative real-time PCR

All RNA was isolated from biofilm (three days). The *S. Mutans* RNA were isolated and purified by using the Ribopure Kit (Life Technology, Grand Island, NY, USA). A NanoPhotometer P360 (Implen, Westlake Village, CA, USA) was used to quantify the total RNA extracted. Reverse transcription of the RNA into cDNA was carried out by using iScript Advanced cDNA synthesis Kit for RT-qPCR (Biorad, Hercules, CA, USA) according to the manufacturer's instructions. Real-time PCR was conducted by using iQ SYBR Green Supermix (Biorad, Hercules, CA, USA) (Klein et al., 2010). The *S. Mutans* primers for the genes: Glucosyltransferase (gtfB), Glucan-binding protein (gpb), at 10 μM were used. The standard curves were used to transform the critical threshold cycle (Ct) values to the relative number of cDNA molecules. Relative expression was calculated by

Table 1 Primers used for RT-qPCR.

GenBank locus tag	Gene name	Primer sequence (forward and reverse)
	16S rRNA	ACCAGAAAGGGACGGCTAAC TAGCCTTTTACTCCAGACTTTCCTG
SMU.1004	gtfB	AAACAACCGAAGCTGATAC CAATTTCTTTTACATTGGGAAG
SMU.22	gbpB	ATACGATTCAAGGACAAGTAAG TGACCCAAAGTAGCAGAC

normalizing each gene of interest to the *S. mutans* 16S rRNA gene, which is a well-established reference gene (Table 1). PCR amplification was performed by using 20 μ L reaction mix per well in a 96 well plate. The reactions were conducted at 95 °C for 3 min, followed by 40 cycles of 15 s at 95 °C and 1 min at 60 °C. After PCR, the melting curve was obtained by incubating the samples at increasing increments of 0.5 °C from 55 to 95 °C (Klein et al., 2009; Koo et al., 2006).

Contact angle–wettability measurement

Wettability of enamel after treatments was evaluated by contact angle measurements. The sessile drop method was performed using Digidrop GBX goniometer (Labometric Lda, Leiria, Portugal) with enamel surface (control and laser). Briefly, deionized water was loaded into a 3 mL syringe (Luer-Lok™ Tip; BD, Franklin Lakes, NJ, USA) and coupled to the goniometer. Droplets (\cong 1 μ L) were carefully applied on the different enamel surfaces using a 22-gauge needle (Injex Ltda, São Paulo, SP, Brazil). Ten drops of water were dispensed on the enamel surface. The measurement of contact angle was accomplished immediately after the water drop has formed on enamel surface. The test was accomplished at room temperature and the drop images captured without external light interferences. Images were frozen by Pixelink system (Barrington, IL, USA) and the measurements were made by the GBX Digidrop Windrop software (GBX Instruments, Bourg de Péage, France). The focus of camera used to capture the images was adjusted in relation to the position of the table with glass slide surface and the needle tip. The right and left angles were measured in degrees of the contact angle and average automatically calculated by GBX Digidrop software (GBX Instruments, Bourg de Péage, France). The average obtained from each specimen and from each group was submitted to statistical analysis (Paris et al., 2007).

Field emission scanning electron microscopy

This analysis aimed to evaluate the surface of specimens after CO₂ LASER irradiation and biofilm formation. All specimens were first mounted on aluminum stubs and sputter-coated with gold (~10–12 nm thickness) using a BAL-TEC SCD 050 sputter coater (Wetzlar, Liechtenstein/Vienna, Austria). Observations were made with a JEOL JSM-7001 Field Emission Scanning Electron Microscope (Jeol, Peabody, MA, USA) operating at 15 kV and using magnifications up to 2500X (Weber et al., 2014).

Table 2 The content of CFU/mL, dry weight (mg/mL), CFU/dry weight in *S. mutans* biofilm. Data represent the mean values and standard deviations.

Groups	Biofilm					
	Day 3			Day 5		
	CFU/mL	Dry weight (mg/mL)	CFU/dry weight	CFU/mL	Dry weight (mg/mL)	CFU/dry weight
Control	8.60 ± 0.33 ^a	6.55 ± 0.37 ^a	7.80 ± 0.31 ^a	7.72 ± 0.29 ^a	10.41 ± 0.92 ^a	6.70 ± 0.29 ^a
Laser	7.78 ± 0.16 ^b	6.70 ± 0.64 ^a	6.99 ± 0.08 ^b	7.67 ± 0.29 ^a	11.38 ± 5.72 ^a	4.31 ± 1.16 ^a

Note:

Means followed by distinct letters (a, b) are statistically different by T-test and Mann-Whitney test. ($p < 0.05$).

Fluorescence microscopy

The distribution of dead and live *S. mutans* was examined after 1, 3 and 5 days of biofilm using the Viability/Cytotoxicity Assay Kit LIVE/DEAD[®] BacLight[™] Bacterial Viability (Life Technologies, Carlsbad, CA, USA) for microscopy which contains a The LIVE/DEAD BacLight Bacterial Viability Kits employ two nucleic acid stains—the green-fluorescent SYTO[®] 9 stain and the red-fluorescent propidium iodide stain. These stains differ in their ability to penetrate healthy bacterial cells. When used alone, SYTO 9 stain labels both live and dead bacteria. In contrast, propidium iodide penetrates only bacteria with damaged membranes, reducing SYTO 9 fluorescence when both dyes are present. Thus, live bacteria with intact green membranes fluoresce, while dead bacteria with damaged membranes fluoresce red were evidenced. Fluorescent images of the double staining were captured using fluorescence microscopy (EVOS fl microscope AMG; Bothell, WA, USA) (Rolland *et al.*, 2006).

Statistical analysis

The Lilliefors test showed that data of CFU, CFU/dry weight on day 3, dry weight on day 5 and insoluble polysaccharide did not follow normal distribution and were analyzed by Mann-Whitney test. Results of adherence test on day 1, dry weight on day 3, CFU, CFU/dry weight on day 5, soluble polysaccharides, real time PCR and contact angle did follow normal distribution and were analyzed by T-test, Data normality and the other analyses were performed using BioEstat 5.0 (Mamirauá, Belém, PA, Brazil) with a 5% significance level.

To evaluate the surface of specimens after treatments and biofilm formation and distribution of dead and live *S. mutans* after one, three and five days of biofilm formation, field emission scanning electron and fluorescence microscopy were respectively performed for illustration.

RESULTS

Table 2 showed, the results of three and five days of biofilm formation. The results on day 3 showed that the values of CFU/mL for irradiated group were significantly ($p < 0.05$) less when compared to the control group. The normalized data (CFU/dry weight) showed noteworthy reduction ($p < 0.05$) by the irradiation on day 3. However, no statistical

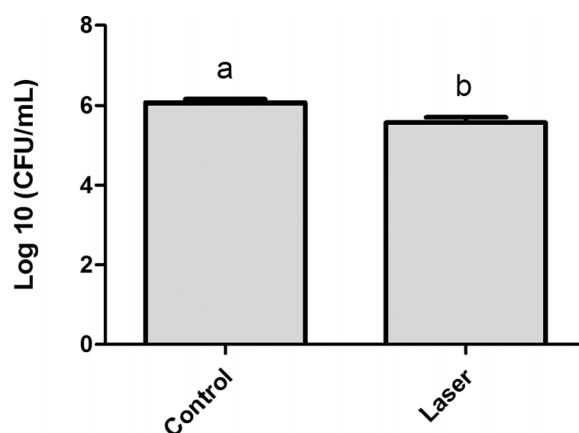


Figure 2 *Streptococcus mutans* adherence test performed in day 1 of biofilm (expressed in log CFU/mL). Values marked by the distinct letters are significantly different from each other. T-test ($p < 0.05$).

Table 3 The content of EPS-soluble, EPS-insoluble in *S. mutans* biofilm (expressed in $\mu\text{g}/\text{mg}$ of biofilm). Data represent the mean values and standard deviations.

Groups	Polysaccharides ($\mu\text{g PSA}/\text{mg dry weight}$)			
	Soluble		Insoluble	
	Day 3	Day 5	Day 3	Day 5
Control	4.92 ± 1.51 ^a	4.89 ± 2.13 ^a	7.20 ± 1.33 ^a	8.84 ± 2.80 ^a
Laser	4.32 ± 1.29 ^a	4.31 ± 1.27 ^a	8.20 ± 2.92 ^a	8.93 ± 1.31 ^a

Note:

Values marked by the different letters (a) are significantly different from each other ($p > 0.05$). T-test was employed for soluble polysaccharide and Mann Whitney test for insoluble polysaccharide.

difference was found between the groups in day 3 for dry weight values ($p > 0.05$).

There were no statistical difference found between the groups in CFU/mL, dry weight and CFU/dry weight on day 5 ($p > 0.05$).

The results obtained for the analysis of *S. mutans* adherence to enamel surface after laser irradiation and biofilm formation are presented in Fig. 2. The values of log CFU/mL obtained for the one-day biofilm evaluation showed that although the difference between the means had been small (control group Log = 6.06 ± 0.23 , irradiated group Log = 5.56 ± 0.35) there is statistical difference between the two groups ($p < 0.05$).

Table 3 showed that soluble and insoluble polysaccharides ($\mu\text{g PSA}/\text{mg dry weight}$) were unaffected by enamel irradiation ($p > 0.05$).

Contact Angle–Wettability Measurement analysis results after enamel treatment were shown in Table 4. This result showed that contact angle was higher for the irradiated group (87.6 ± 9.41) than for the control group (76.0 ± 3.33) and the difference between the two groups was statistically significant ($p < 0.05$).

To assess the effect of CO₂ laser irradiated surface on *S. mutans* gene expression we used quantitative real time PCR. We compared control non-irradiated samples to irradiated samples. The difference in the genes expression (gtfB and gbpB) was not statically significant (Fig. 3).

Table 4 The content of contact angle, mutans biofilm. Data represent the mean values of angle ($^{\circ}$) and standard deviations.

Groups	Contact angle ($^{\circ}$)
Control	76.0 ± 3.33^a
Laser	87.6 ± 9.41^b

Note:

Values marked by the different letters (a, b) are significantly different from each other. T-test ($p < 0.05$).

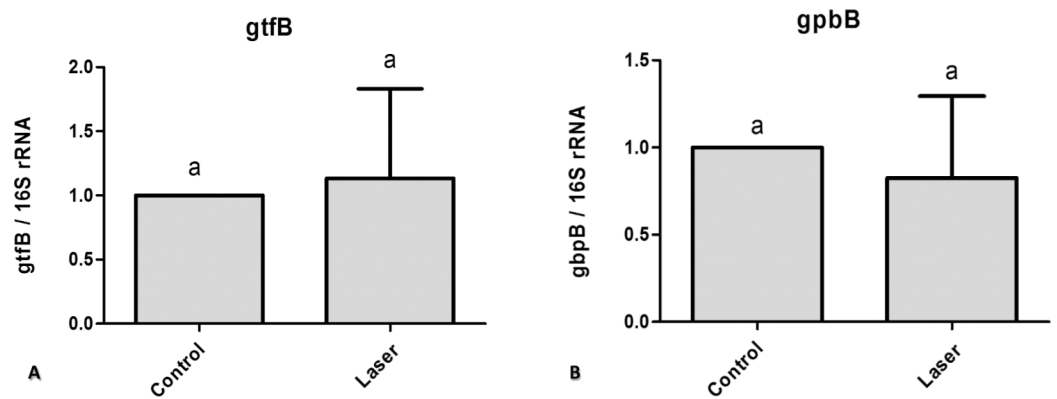


Figure 3 Real time quantitative information about gene expression in *S. mutans* biofilm after treatments with/without laser irradiation on enamel surface. (A) gtffB (B) gpbB. Values marked by the same letters are not significantly different from each other ($p > 0.05$). T-test ($p > 0.05$).

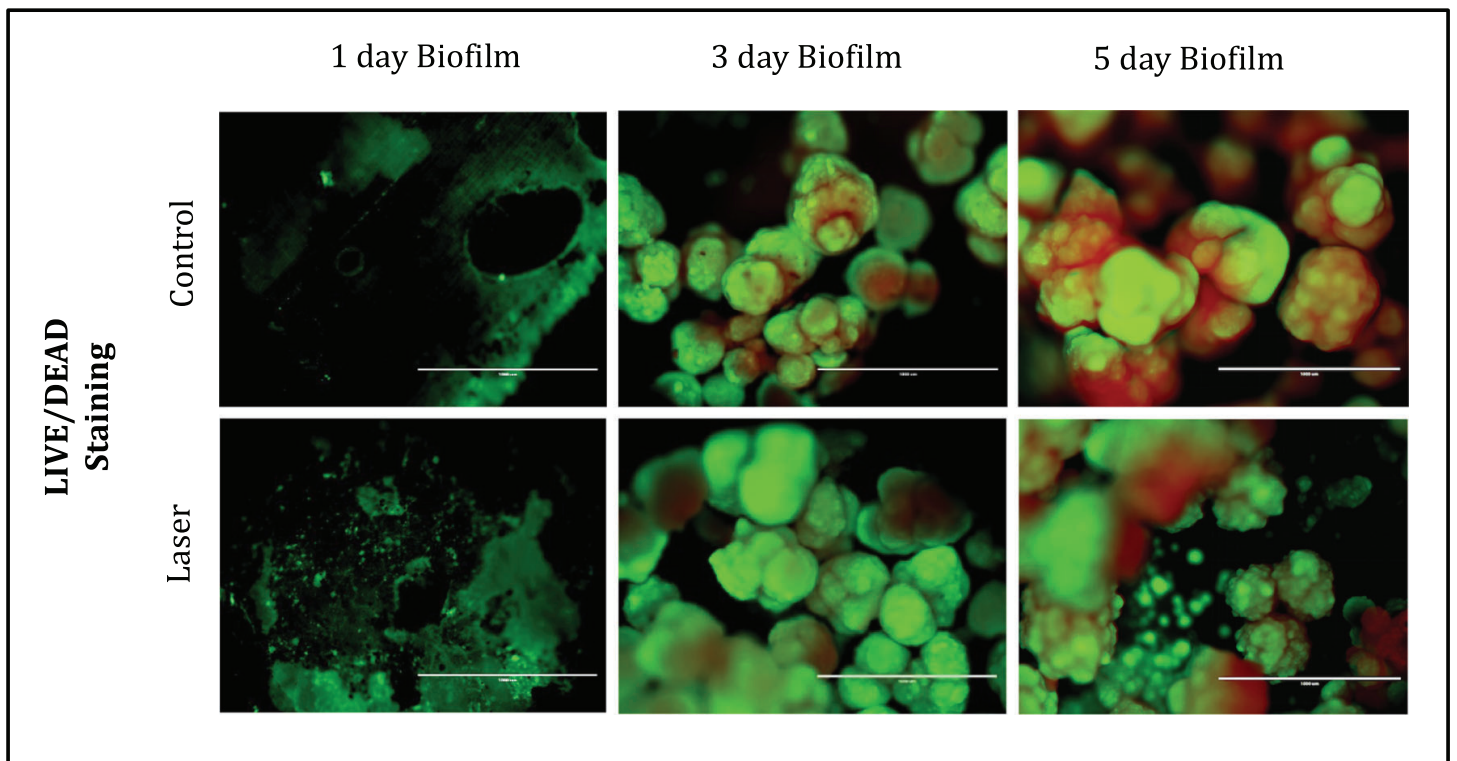


Figure 4 Fluorescence Microscopy showing representative images of bacteria in biofilms after 1, 3 and 5 days of biofilm. Multidimensional imaging of live (green) and dead (red) bacteria.

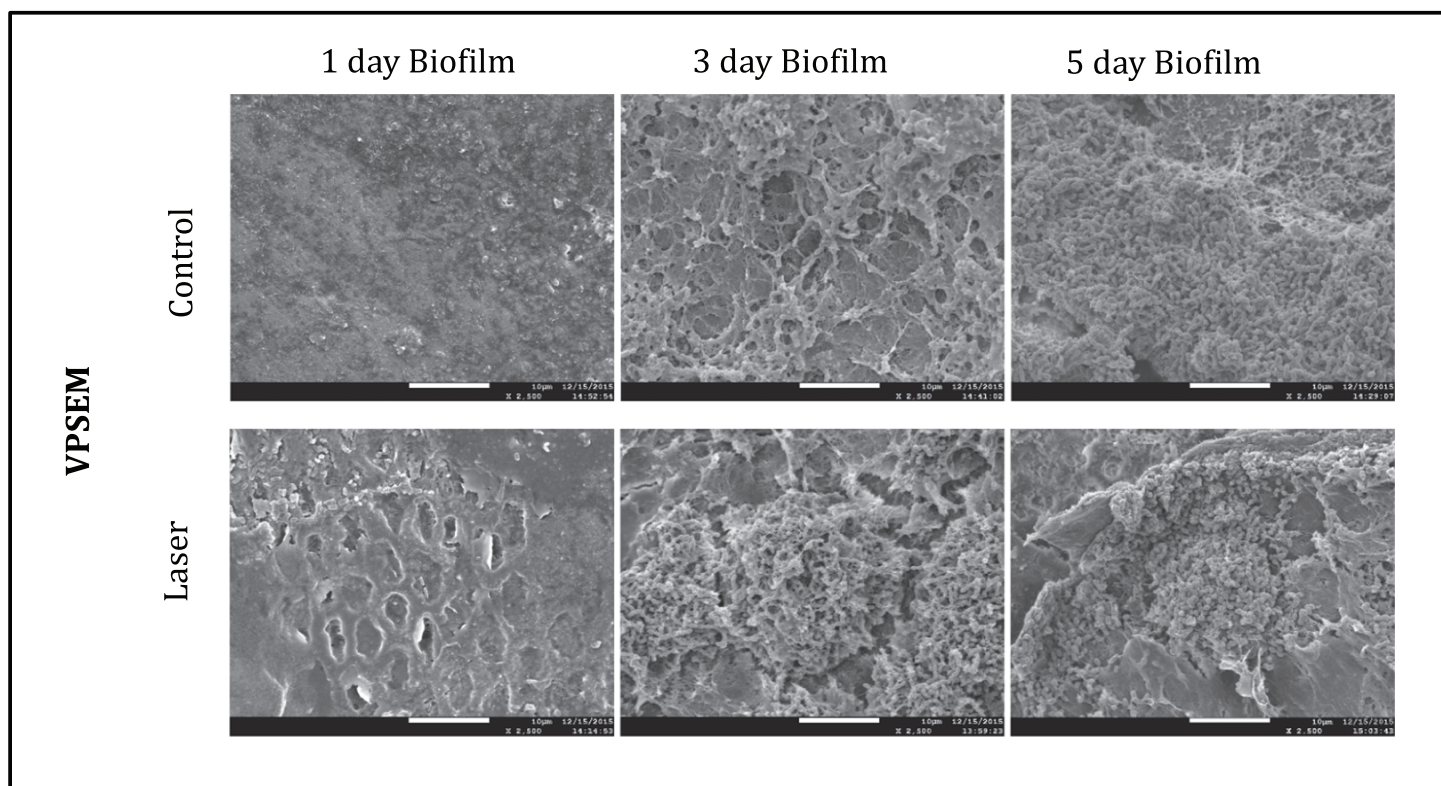


Figure 5 Morphology and structure of after one, three and five days *S. mutans* biofilms imaged by FESEM (2500X).

Fluorescence Microscopy representative images of bacteria in biofilms after one, three and five days of biofilm were shown in Fig. 4. Multidimensional imaging of live (Green) and dead (red) bacteria can be observed at different times of *S. mutans* biofilm. Similar results were found in both groups of treatment. Biofilms formed on specimens became denser from day 1 to day 5. The image on day 1 showed primarily few amounts of live bacteria, with no dead cells. In contrast, substantial increases in dead bacteria occurred with the increase of the days. In the last day (day 5), biofilms consisted of primarily dead bacteria, connected with each other to form twisted strings. Another aspect that is possible to observe is that on day 3 the dead cells (red) were located inside the biofilm while the live cells were externalized, but on day 5 the predominance of dead cells occurred.

The SEM images of each group at different time points were shown in Fig. 5. The images illustrated the effects of enamel CO₂ laser irradiation on the morphology and structure on *S. mutans* biofilm. On day 1, both groups had less bacteria in the biofilm than the day 3 and 5. Specimens with five days biofilm presented a thick and dense biofilm. Irradiated group had biofilms similar to those of composite control in both days. However, on day 1, the SEM observation revealed evidence of melting and fusion in the specimens treated with the CO₂ laser.

DISCUSSION

Laser irradiation has long been used in medicine and lately also in the dental field. Some of these applications are intended for areas where bacteria are harbored or used directly

to eradicate bacteria from infected areas (*Sol et al., 2011*). Another aspect to consider is that the critical pH (5.5) for the dissolution of enamel is reduced to 4.8 after irradiation with CO₂ laser (*Fox et al., 1992*). Despite a variety of experiments demonstrating the inhibitory effect of CO₂ laser in reducing enamel demineralization, little is known about the effect of surface irradiation on bacterial growth.

The wavelengths obtained with CO₂ lasers ($\lambda = 9.3, 9.6, 10.3$ and $10.6 \mu\text{M}$) produce radiation in the infrared region, which coincides with some absorption bands of hydroxyapatite, particularly the carbonate and phosphate groups (*Rodrigues, dos Santos & Featherstone, 2006*). When the light is absorbed in a few external micrometers from the surface of the tooth and converted the enamel, a heat loss occurs in mineral carbonate as well as fusion of the hydroxyapatite crystals, resulting in a decrease of acid reactivity in this structure (*Fried et al., 1997*). The reduced solubility of spent enamel has also been attributed to melting and recrystallization of the crystals (*Nelson et al., 1986; Nelson et al., 1987*). These morphological changes can interfere in the default adhesion of bacterial cells to the tooth surface, which is essential to early carious lesions formation (*Newbrun, 1977*).

Adhesion is the initial step in biofilm formation. Thus, an understanding of bacteria-surface interactions is essential for biofilm control. Bacterial cells approach surfaces by different means, including sedimentation, movement with liquid flow, bacterial motility with cell surface appendages, and interaction with other cells to form aggregates (*Teughels et al., 2006*). In this study, initial adhesion in day 1 of biofilm formation was investigated and the data revealed that laser irradiation decreased the initial cell adherence of *Streptococcus mutans*. On day 3, it is possible to observe a greater value of biofilm formation in control group. However, with the progression of time, at day 5, this difference becomes less visible and is statistically similar.

The formation and composition of biofilm appear to vary on different surfaces (*Aroonsang et al., 2014*) and effects of material/surface properties, such as surface charge, hydrophobicity, roughness, topography, and chemistry on bacterial adhesion and biofilm formation have been investigated for many years (*Anselme et al., 2010; Badihi Hauslich et al., 2013; Guégan et al., 2014; Perera-Costa et al., 2014; Song & Ren, 2014*). These factors may be interrelated, which may explain the inhibition of biofilm formation found on irradiated enamel.

The role of hydrophobicity in oral bacterial adhesion has been reviewed elsewhere (*Busscher, Norde & van der Mei, 2008; Busscher et al., 2010; Nobbs, Lamont & Jenkinson, 2009*). In general, by tuning the hydrophobicity of a surface, bacterial adhesion can be inhibited. The results of this present study indicated that laser irradiation was able to increase the hydrophobicity of the enamel when compared to the control group. This finding was in agreement with a previous report by *Quiryne et al. (1996)*, who showed that in oral environments on supragingival surfaces, less biofilm is formed on hydrophobic surfaces than hydrophilic ones. This increase of the hydrophobicity on irradiated enamel can be related to the decrease in initial biofilm formation which was found in this study.

Gene expression in bacteria can be affected by light and laser irradiation (*Steinberg et al., 2008*). However, how bacteria sense and respond to different surface properties at

the genetic level is largely unknown. *S. mutans* does not always dominate within dental plaque, but it is recognized that glucosyltransferases (Gtfs) from *S. mutans* play critical roles in the development of virulent dental plaque. These Gtf genes, among other functions, are responsible for producing the soluble and insoluble polysaccharides matrix. The EPS-insoluble plays a significant role on *S. mutans* adhesion and accumulation on the tooth surface (Bowen & Koo, 2011). In addition, it potentially changes the biofilm structure, resulting in increased porosity (Dibdin & Shellis, 1988), which allows fermentable substrates to diffuse and be metabolized in the deepest parts of the biofilm (Zero, van Houte & Russo, 1986). The present study demonstrated that irradiating enamel surface with laser irradiation did not affect the gene expression of GtfB and, consequently, did not change the production of polysaccharides. Conversely, synthesis of glucan binding proteins (Gbps) may enhance the ability of *S. mutans* to interact with the EPS-rich matrix (Banas & Vickerman, 2003). The adhesion between the bacterial cells and the EPS-matrix may be partially mediated by cell-surface GbpC, and possibly GbpB whereas secreted GbpA and GbpD may be cross-linked with the matrix contributing to the maintenance of the biofilm architecture (Lynch et al., 2007). The amounts of GbpB observed in irradiated enamel do not have direct implications for the biofilm morphogenesis and structural integrity (Duque et al., 2011).

To determine the morphology of *S. mutans* biofilms with respect to topography, we used SEM microscopy. In our study, the *S. mutans* biofilm topography was visibly not altered after laser irradiation, in both fluorescence microscopy and SEM images. This result suggests that although the laser irradiation promoted surfaces alteration such as fusion and melt, which is visible in MEV it did not promote disorganization and disaggregation of the microorganisms in the biofilm, inhibiting their growth and metabolism.

To the best of our knowledge, this is the first report of CO₂ laser irradiation effect on the prevention of oral biofilm development. Laser irradiation modified *S. mutans* biofilm development by reducing its formation. Our findings suggest that bacteria have complex systems to sense and respond to environmental challenges. The interplay between how surface properties and pellicle formation affect the bacterial adhesion strength, the mechanical stability, and detachment of biofilms, is an area that needs to be elucidated. In conclusion, CO₂ laser irradiation can modify the energy surface and disrupt the initial biofilm formation.

ACKNOWLEDGEMENTS

Dr. Carolina Steiner-Oliveira at Piracicaba Dental School, University of Campinas and Dr. Patricia Moreira de Freitas at School of Dentistry, University of São Paulo are sincerely thanked for their input into the study.

ADDITIONAL INFORMATION AND DECLARATIONS

Funding

Research reported in this publication was supported by the National Center for Complementary and Integrative Health of the National Institutes of Health under award

number R00AT006507, CAPES Foundation (Process No. 2339-15-3) and FAPESP (Process No. 2012/02885-7) from whom the first author received a scholarship. The funders had no role in study design, data collection and analysis, decision to publish, or preparation of the manuscript.

Grant Disclosures

The following grant information was disclosed by the authors:

National Center for Complementary and Integrative Health of the National Institutes of Health: R00AT006507.

CAPES Foundation: 2339-15-3.

FAPESP: 2012/02885-7.

Competing Interests

The authors declare that they have no competing interests.

Author Contributions

- Bruna Raquel Zancopé conceived and designed the experiments, performed the experiments, analyzed the data, contributed reagents/materials/analysis tools, wrote the paper, prepared figures and/or tables, reviewed drafts of the paper.
- Vanessa B. Dainezi performed the experiments, analyzed the data, contributed reagents/materials/analysis tools.
- Marinês Nobre-dos-Santos conceived and designed the experiments, analyzed the data, contributed reagents/materials/analysis tools, wrote the paper, prepared figures and/or tables, reviewed drafts of the paper.
- Sillas Duarte Jr. performed the experiments, analyzed the data, contributed reagents/materials/analysis tools, prepared figures and/or tables.
- Vanessa Pardi analyzed the data, contributed reagents/materials/analysis tools, wrote the paper, prepared figures and/or tables, reviewed drafts of the paper.
- Ramiro M. Murata conceived and designed the experiments, performed the experiments, analyzed the data, contributed reagents/materials/analysis tools, wrote the paper, prepared figures and/or tables, reviewed drafts of the paper.

Data Deposition

The following information was supplied regarding data availability:

The raw data has been supplied as [Supplemental Dataset Files](#).

Supplemental Information

Supplemental information for this article can be found online at <http://dx.doi.org/10.7717/peerj.2458#supplemental-information>.

REFERENCES

- Anselme K, Davidson P, Popa AM, Giazon M, Liley M, Ploux L. 2010. The interaction of cells and bacteria with surfaces structured at the nanometre scale. *Acta Biomaterialia* 6(10):3824–3846 DOI 10.1016/j.actbio.2010.04.001.

- Armengol V, Laboux O, Weiss P, Jean A, Hamel H. 2003. Effects of Er:YAG and Nd:YAP laser irradiation on the surface roughness and free surface energy of enamel and dentin: an in vitro study. *Operative Dentistry* 28(1):67–74.
- Aroonsang W, Sotres J, El-Schich Z, Arnebrant T, Lindh L. 2014. Influence of substratum hydrophobicity on salivary pellicles: organization or composition? *Biofouling* 30(9):1123–1132 DOI 10.1080/08927014.2014.974155.
- Badihi Hauslich L, Sela MN, Steinberg D, Rosen G, Kohavi D. 2013. The adhesion of oral bacteria to modified titanium surfaces: role of plasma proteins and electrostatic forces. *Clinical Oral Implants Research* 24(Suppl A100):49–56 DOI 10.1111/j.1600-0501.2011.02364.x.
- Banas JA, Vickerman MM. 2003. Glucan-binding proteins of the oral streptococci. *Critical Reviews in Oral Biology & Medicine* 14(2):89–99 DOI 10.1177/154411130301400203.
- Bowen WH. 2002. Do we need to be concerned about dental caries in the coming millennium? *Critical Reviews in Oral Biology & Medicine* 13(2):126–131 DOI 10.1177/154411130201300203.
- Bowen WH, Koo H. 2011. Biology of Streptococcus mutans-derived glucosyltransferases: role in extracellular matrix formation of cariogenic biofilms. *Caries Research* 45(1):69–86 DOI 10.1159/000324598.
- Branco-de-Almeida LS, Murata RM, Franco EM, dos Santos MH, de Alencar SM, Koo H, Rosalen PL. 2011. Effects of 7-epiclusianone on Streptococcus mutans and caries development in rats. *Planta Medica* 77(1):40–45 DOI 10.1055/s-0030-1250121.
- Buergers R, Schneider-Brachert W, Hahnel S, Rosentritt M, Handel G. 2009. Streptococcal adhesion to novel low-shrink silorane-based restorative. *Dental Materials* 25(2):269–275 DOI 10.1016/j.dental.2008.07.011.
- Busscher HJ, Norde W, van der Mei HC. 2008. Specific molecular recognition and nonspecific contributions to bacterial interaction forces. *Applied and Environmental Microbiology* 74(9):2559–2564 DOI 10.1128/AEM.02839-07.
- Busscher HJ, Rinastiti M, Siswomihardjo W, van der Mei HC. 2010. Biofilm formation on dental restorative and implant materials. *Journal of Dental Research* 89(7):657–665 DOI 10.1177/0022034510368644.
- Dibdin GH, Shellis RP. 1988. Physical and biochemical studies of Streptococcus mutans sediments suggest new factors linking the cariogenicity of plaque with its extracellular polysaccharide content. *Journal of Dental Research* 67(6):890–895 DOI 10.1177/00220345880670060101.
- Do LG. 2012. Distribution of caries in children: variations between and within populations. *Journal of Dental Research* 91(6):536–543 DOI 10.1177/0022034511434355.
- Duarte S, Gregoire S, Singh AP, Vorsa N, Schaich K, Bowen WH, Koo H. 2006. Inhibitory effects of cranberry polyphenols on formation and acidogenicity of Streptococcus mutans biofilms. *FEMS Microbiology Letters* 257(1):50–56 DOI 10.1111/j.1574-6968.2006.00147.x.
- Duarte S, Kuo SP, Murata RM, Chen CY, Saxena D, Huang KJ, Popovic S. 2011. Air plasma effect on dental disinfection. *Physics of Plasmas* 18(7):073503 DOI 10.1063/1.3606486.
- Dubois M, Gilles K, Hamilton JK, Rebers PA, Smith F. 1951. A colorimetric method for the determination of sugars. *Nature* 168(4265):167 DOI 10.1038/168167a0.
- Duque C, Stipp RN, Wang B, Smith DJ, Höfling JE, Kuramitsu HK, Duncan MJ, Mattos-Graner RO. 2011. Downregulation of GbpB, a component of the VicRK regulon, affects biofilm formation and cell surface characteristics of Streptococcus mutans. *Infection and Immunity* 79(2):786–796 DOI 10.1128/IAI.00725-10.
- Dye BA, Nowjack-Raymer R, Barker LK, Nunn JH, Steele JG, Tan S, Lewis BG, Beltran-Aguilar ED. 2008. Overview and quality assurance for the oral health component of

- the National Health and Nutrition Examination Survey (NHANES), 2003–04. *Journal of Public Health Dentistry* **68**(4):218–226 DOI [10.1111/j.1752-7325.2007.00076.x](https://doi.org/10.1111/j.1752-7325.2007.00076.x).
- Featherstone JDB, Zhang SH, Shariati M, McCormack SM. 1991.** Carbon dioxide laser effects on caries-like lesions of dental enamel. *Proceedings of SPIE—Lasers in Orthopedic, Dental, and Veterinary Medicine, Los Angeles*, **1424**:145.
- Featherstone JDB, Barrett-Vespone NA, Fried D, Kantorowitz Z, Seka W. 1998.** CO₂ laser inhibitor of artificial caries-like lesion progression in dental enamel. *Journal of Dental Research* **77**(6):1397–1403 DOI [10.1177/00220345980770060401](https://doi.org/10.1177/00220345980770060401).
- Fox JL, Yu D, Otsuka M, Higuchi WI, Wong J, Powell G. 1992.** Combined effects of laser irradiation and chemical inhibitors on the dissolution of dental enamel. *Caries Research* **26**(5):333–339 DOI [10.1159/000261464](https://doi.org/10.1159/000261464).
- Fried D, Glana RE, Featherstone JDB, Seka W. 1997.** Permanent and transient changes in the reflectance of CO₂ laser-irradiated dental hard tissues at $\lambda = 9.3, 9.6, 10.3,$ and $10.6 \mu\text{m}$ and at fluences of $1\text{--}20 \text{ J/cm}^2$. *Lasers in Surgery and Medicine* **20**(1):22–31 DOI [10.1002/\(SICI\)1096-9101\(1997\)20:1<22::AID-LSM4>3.0.CO;2-0](https://doi.org/10.1002/(SICI)1096-9101(1997)20:1<22::AID-LSM4>3.0.CO;2-0).
- García-Godoy F, Hicks MJ. 2008.** Maintaining the integrity of the enamel surface: the role of dental biofilm, saliva and preventive agents in enamel demineralization and remineralization. *Journal of the American Dental Association* **139**(Suppl 2):25S–34S DOI [10.14219/jada.archive.2008.0352](https://doi.org/10.14219/jada.archive.2008.0352).
- Greene VA. 2005.** Underserved elderly issues in the United States: burdens of oral and medical health care. *Dental Clinics of North America* **49**(2):363–376 DOI [10.1016/j.cden.2004.11.001](https://doi.org/10.1016/j.cden.2004.11.001).
- Guégan C, Garderes J, Le Pennec G, Gaillard F, Fay F, Linossier I, Herry J-M, Fontaine M-N, Réhel KV. 2014.** Alteration of bacterial adhesion induced by the substrate stiffness. *Colloids and Surfaces B: Biointerfaces* **114**:193–200 DOI [10.1016/j.colsurfb.2013.10.010](https://doi.org/10.1016/j.colsurfb.2013.10.010).
- Hausen H. 1997.** Caries prediction—state of the art. *Community Dentistry and Oral Epidemiology* **25**(1):87–96 DOI [10.1111/j.1600-0528.1997.tb00904.x](https://doi.org/10.1111/j.1600-0528.1997.tb00904.x).
- Hsu C-YS, Jordan TH, Dederich DN, Wefel JS. 2000.** Effects of low-energy CO₂ laser irradiation and the organic matrix on inhibition of enamel demineralization. *Journal of Dental Research* **79**(9):1725–1730 DOI [10.1177/00220345000790091401](https://doi.org/10.1177/00220345000790091401).
- Hsu C-YS, Jordan TH, Dederich DN, Wefel JS. 2001.** Laser-matrix-fluoride effects on enamel demineralization. *Journal of Dental Research* **80**(9):1797–1801 DOI [10.1177/00220345010800090501](https://doi.org/10.1177/00220345010800090501).
- Kantorowitz Z, Featherstone JDB, Fried D. 1998.** Caries prevention by CO₂ laser treatment: dependency on the number of pulses used. *Journal of the American Dental Association* **129**(5):585–591 DOI [10.14219/jada.archive.1998.0276](https://doi.org/10.14219/jada.archive.1998.0276).
- Klein MI, DeBaz L, Agidi S, Lee H, Xie G, Lin AH-M, Hamaker BR, Lemos JA, Koo H. 2010.** Dynamics of *Streptococcus mutans* transcriptome in response to starch and sucrose during biofilm development. *PLoS ONE* **5**(10):e13478 DOI [10.1371/journal.pone.0013478](https://doi.org/10.1371/journal.pone.0013478).
- Klein MI, Duarte S, Xiao J, Mitra S, Foster TH, Koo H. 2009.** Structural and molecular basis of the role of starch and sucrose in *Streptococcus mutans* biofilm development. *Applied and Environmental Microbiology* **75**(3):837–841 DOI [10.1128/AEM.01299-08](https://doi.org/10.1128/AEM.01299-08).
- Koo H, Seils J, Abranches J, Burne RA, Bowen WH, Quivey RG. 2006.** Influence of apigenin on *gtf* gene expression in *Streptococcus mutans* UA159. *Antimicrobial Agents and Chemotherapy* **50**(2):542–546 DOI [10.1128/AAC.50.2.542-546.2006](https://doi.org/10.1128/AAC.50.2.542-546.2006).
- Loesche WJ. 1986.** Role of *Streptococcus mutans* in human dental decay. *Microbiological Reviews* **50**(4):353–380.

- Lynch DJ, Fountain TL, Mazurkiewicz JE, Banas JA. 2007. Glucan-binding proteins are essential for shaping *Streptococcus mutans* biofilm architecture. *FEMS Microbiology Letters* 268(2):158–165 DOI 10.1111/j.1574-6968.2006.00576.x.
- Marcenes W, Kassebaum NJ, Bernabe E, Flaxman A, Naghavi M, Lopez A, Murray CJL. 2013. Global burden of oral conditions in 1990–2010: a systematic analysis. *Journal of Dental Research* 92(7):592–597 DOI 10.1177/0022034513490168.
- Marsh PD. 2003. Are dental diseases examples of ecological catastrophes? *Microbiology* 149(2):279–294 DOI 10.1099/mic.0.26082-0.
- Murata RM, Branco-de-Almeida LS, Franco EM, Yatsuda R, dos Santos MH, de Alencar SM, Koo H, Rosalen PL. 2010. Inhibition of *Streptococcus mutans* biofilm accumulation and development of dental caries in vivo by 7-epiclusianone and fluoride. *Biofouling* 26(7):865–872 DOI 10.1080/08927014.2010.527435.
- Murata RM, Pardi V. 2007. Is dental caries reaching epidemic proportions in Brazil? *Nature Reviews Immunology* 7(4):1 DOI 10.1038/nri1857-c1.
- Nelson DGA, Shariati M, Glana R, Shields CP, Featherstone JDB. 1986. Effect of pulsed low energy infrared laser irradiation on artificial caries-like lesion formation. *Caries Research* 20(4):289–299 DOI 10.1159/000260948.
- Nelson DGA, Wefel JS, Jongebloed WL, Featherstone JDB. 1987. Morphology, histology and crystallography of human dental enamel treated with pulsed low-energy infrared laser radiation. *Caries Research* 21(5):411–426 DOI 10.1159/000261047.
- Newbrun E. 1977. Control of dental caries. *Southern Medical Journal* 70(10):1161–1114.
- Nobbs AH, Lamont RJ, Jenkinson HF. 2009. Streptococcus adherence and colonization. *Microbiology and Molecular Biology Reviews* 73(3):407–450 DOI 10.1128/MMBR.00014-09.
- Nobre-dos-Santos M, Featherstone JDB, Fried D. 2001. Effect of a new carbon dioxide laser and fluoride on sound and demineralized enamel. *Proceedings of SPIE—International Society for Optical Engineering, San Jose*, 4249:169–174 DOI 10.1117/12.424504.
- Paris S, Meyer-Lueckel H, Cölfen H, Kielbassa AM. 2007. Penetration coefficients of commercially available and experimental composites intended to infiltrate enamel carious lesions. *Dental Materials* 23(6):742–748 DOI 10.1016/j.dental.2006.06.029.
- Peterson PE. 2003. The world oral health report 2003. Continuous improvement of oral health in the 21st century—the approach of the WHO global oral health programme. Geneva: World Health Organization.
- Perera-Costa D, Bruque JM, González-Martín ML, Gómez-García AC, Vadillo-Rodríguez V. 2014. Studying the influence of surface topography on bacterial adhesion using spatially organized microtopographic surface patterns. *Langmuir* 30(16):4633–4641 DOI 10.1021/la5001057.
- Quirynen M, Bollen CML, Papaioannou W, Van Eldere J, van Steenberghe D. 1996. The influence of titanium abutment surface roughness on plaque accumulation and gingivitis: short-term observations. *International Journal of Oral & Maxillofacial Implants* 11(2):169–178.
- Rodrigues LKA, Norbe dos Santos M, Featherstone JD. 2006. In situ mineral loss inhibition by CO₂ laser and fluoride. *Journal of Dental Research* 85(7):617–621 DOI 10.1177/154405910608500707.
- Rölla G. 1989. Why is sucrose so cariogenic? The role of glucosyltransferase and polysaccharides. *Scandinavian Journal of Dental Research* 97(2):115–119.
- Rolland SL, McCabe JF, Robinson C, Walls AWG. 2006. In vitro biofilm formation on the surface of resin-based dentine adhesives. *European Journal of Oral Sciences* 114(3):243–249 DOI 10.1111/j.1600-0722.2006.00359.x.

- Sol A, Feuerstein O, Featherstone JDB, Steinberg D. 2011.** Effect of sublethal CO₂ laser irradiation on gene expression of streptococcus mutans immobilized in a biofilm. *Caries Research* 45(4):361–369 DOI 10.1159/000329390.
- Song F, Ren D. 2014.** Stiffness of cross-linked poly(dimethylsiloxane) affects bacterial adhesion and antibiotic susceptibility of attached cells. *Langmuir* 30(34):10354–10362 DOI 10.1021/la502029f.
- Steinberg D, Moreinos D, Featherstone J, Shemesh M, Feuerstein O. 2008.** Genetic and physiological effects of noncoherent visible light combined with hydrogen peroxide on Streptococcus mutans in biofilm. *Antimicrobial Agents and Chemotherapy* 52(7):2626–2631 DOI 10.1128/AAC.01666-07.
- Steiner-Oliveira C, Rodrigues LKA, Soares LES, Martin AA, Zezell DM, Nobre-dos-Santos M. 2006.** Chemical, morphological and thermal effects of 10.6 μm CO₂ laser on the inhibition of enamel demineralization. *Dental Materials Journal* 25(3):455–462 DOI 10.4012/dmj.25.455.
- Tagliaferro EPS, Rodrigues LKA, Nobre Dos Santos M, Soares LES, Martin AA. 2007.** Combined effects of carbon dioxide laser and fluoride on demineralized primary enamel: an in vitro study. *Caries Research* 41(1):74–76 DOI 10.1159/000096109.
- Taubman MA, Nash DA. 2006.** The scientific and public-health imperative for a vaccine against dental caries. *Nature Reviews Immunology* 6(7):555–563 DOI 10.1038/nri1857.
- Teughels W, Van Assche N, Sliepen I, Quirynen M. 2006.** Effect of material characteristics and/or surface topography on biofilm development. *Clinical Oral Implants Research* 17(Suppl S2):68–81 DOI 10.1111/j.1600-0501.2006.01353.x.
- Venault A, Yang H-S, Chiang Y-C, Lee B-S, Ruaan R-C, Chang Y. 2014.** Bacterial resistance control on mineral surfaces of hydroxyapatite and human teeth via surface charge-driven antifouling coatings. *ACS Applied Materials & Interfaces* 6(5):3201–3210 DOI 10.1021/am404780w.
- Wang Q, Jia P, Cuenco KT, Feingold E, Marazita ML, Wang L, Zhao Z. 2013.** Multi-dimensional prioritization of dental caries candidate genes and its enriched dense network modules. *PLoS ONE* 8(10):e76666 DOI 10.1371/journal.pone.0076666.
- Weber K, Delben J, Bromage TG, Duarte S. 2014.** Comparison of SEM and VPSEM imaging techniques with respect to *Streptococcus mutans* biofilm topography. *FEMS Microbiology Letters* 350(2):175–179 DOI 10.1111/1574-6968.12334.
- Zero DT, van Houte J, Russo J. 1986.** Enamel demineralization by acid produced from endogenous substrate in oral Streptococci. *Archives of Oral Biology* 31(4):229–234 DOI 10.1016/0003-9969(86)90054-3.